Hybrid Reconstruction Method for Flow-Sensitive Dephasing Non-contrast MRA

A. J. Wheaton[1], and M. Miyazaki[2]

[1]Toshiba Medical Research Institute USA, Mayfield, OH, United States, [2]Toshiba Medical Research Institute USA, Vernon Hills, IL, United States

INTRODUCTION

Flow-sensitive dephasing (FSD) is a non-contrast MRA technique based on the acquisition of two separate image sets: bright artery (BA) and dark artery (DA) (1-2). The flow-sensitivity of each image set is controlled by adjusting the first moment (m1) of a motion-sensitive dephasing (MSDE) prepulse module (3). The BA and DA data are then subtracted to create an (ideally) arteries-only data set.

The value of m1 for the FSD BA and DA scans must be carefully calibrated (2). If m1 is too low, arteries will not be fully attenuated, especially for slow flow arteries. Hence, their pixel values will be reduced in the final BA–DA subtraction image. Likewise, if m1 is too high, venous flow can also be attenuated in the DA image. Any venous attenuation results in contamination at the venous pixel locations in the BA–DA subtraction image.

The degree of MSDE signal attenuation is sinusoidally proportional to the product of m1 and flow velocity (Figure 1) (4). Arteries generally have higher flow velocities and are more strongly influenced by the pulsatile effects of the cardiac cycle compared to veins. Hence, arteries are expected to experience greater signal attenuation than veins, even more so during systole.

PURPOSE

The purpose of this study is to develop a hybrid FSD reconstruction algorithm to generate noncontrast FSD images with optimal artery to background contrast while avoiding contamination from veins by using *a priori* knowledge of the relationship between signal intensity and m1 / cardiac cycle in arteries and veins.

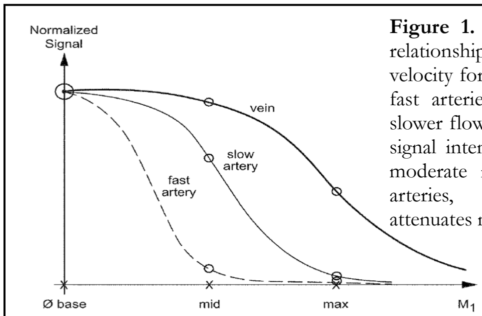

Figure 1. Illustration of general relationship between m1 and flow velocity for veins, slow arteries, and fast arteries. Veins generally have slower flow and thus maintain their signal intensity in the presence of moderate m1. For fast velocity arteries, even moderate m1 attenuates most of the signal.

HYBRID RECONSTRUCTION ALGORITHM

The hybrid reconstruction algorithm uses multiple (N ≥ 2) FSD data sets as input. In the example in Fig 1, N=3 image sets are acquired: "base" @ m1=off [in diastole], "mid" @ m1 = middle value [in systole], and "max" @ m1=high [in systole].

Instead of a simple subtraction (BA-DA), the pixel data from each of the N data sets is input into a combination algorithm to create a hybrid image set *X* (Figure 2A). The hybrid image set *X* is created using pixel data from the N data sets and used in the subtraction to create the final MRA image *I*. Inside the combination algorithm, the pixel data are compared against each other to make an intelligent guess as to whether each pixel is part of an artery or vein. This decision is based on *a priori* knowledge of the relative flow rate and pulsatility according to Figure 1. An example combination algorithm is described in Figure 2B.

METHODS

The lower legs of a male volunteer were scanned on a 3T whole-body research system under IRB approval. The MSDE module was appended to a partial Fourier 3D FSE sequence. Image parameters include: 36 slices, 3 mm thick, FOV = 35 x 35 cm, matrix = 256 x 256, echo space = 5 ms, TE = 30 ms, ETL = 70, 2 shots. Peripheral pulse gating was used with 2 RR intervals (~2000ms) for a total acquisition time of 2:30 per image set. Three image sets were acquired at the m1/cardiac phase positions indicated on Figure 1. The nonzero values of m1 (expressed in terms of VENC) were: 80 cm/sec, and 15 cm/sec for mid and max data sets, respectively. Simple FSD subtractions were performed (base–mid and base–max) as well as the hybrid reconstruction using the algorithm diagrammed in Figure 2 using ε = 0.5. Coronal MIP images were constructed from each post-subtraction data set.

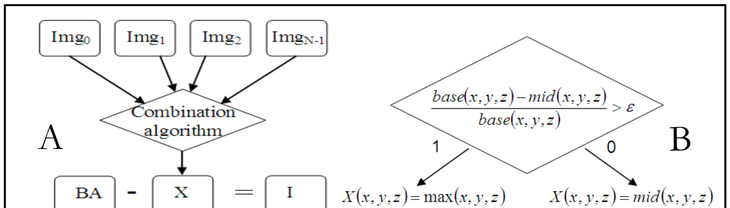

Figure 2. Diagram of hybrid reconstruction algorithm. A) N images are combined to create hybrid image X which is used in the subtraction. B) Example of combination algorithm for N = 3 data sets described in Methods and Figure 1.

RESULTS & DISCUSSION

The hybrid reconstruction method produced increased arterial signal and reduced venous contamination compared to simple subtraction (Figures 3 and 4). The improvement in arterial signal (up to 100%) was heterogeneous with the most prevalent increases in areas with slower flow, including the smaller vessels below the trifurcation and near vessel walls. Venous contamination was reduced to near zero. The reduction in venous contamination is especially important considering arteries and veins generally run alongside each other in peripheral anatomy.

This study was conducted on a healthy volunteer. Thus, the design and/or tuning (ε) of the decision algorithm (Figure 2B) may need to be modified to accommodate flow patterns in symptomatic individuals. Since the hybrid reconstruction can be repeatedly executed on the same acquired data, it is possible to generate multiple outputs from which a user-directed decision can be made. For example, a series of MIP images can be created for a corresponding series of ε values.

CONCLUSION: The hybrid reconstruction FSD algorithm incorporates *a priori* knowledge to generate MRA images with bright arterial signal, even in slow flow arteries, and minimal venous contamination.

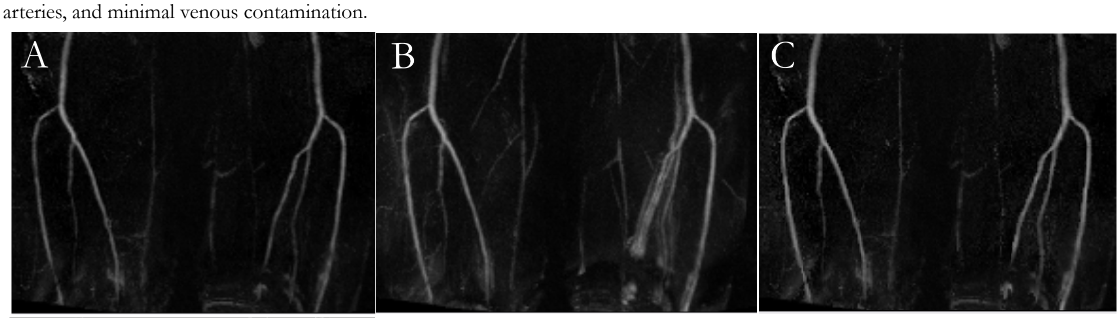

Figure 3. Comparison of MIP images created with A) base-mid, B) base-max, and C) hybrid method. For clarity, only the lower portion of the FOV, including the trifurcation and below, is displayed.

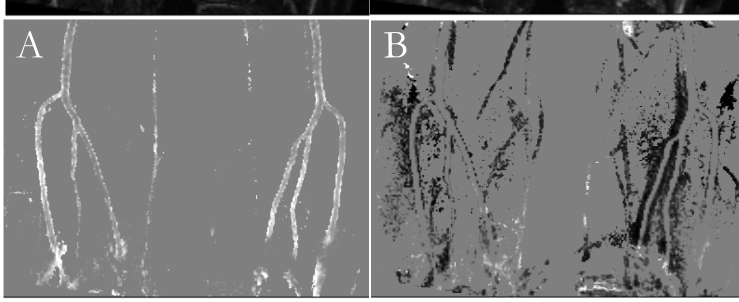

Figure 4. Improvement of hybrid reconstruction vs. simple subtraction. In both images, gray represents no change. A) Increase in signal intensity of hybrid data (Fig 3C) vs. base-mid data (Fig 3A). Here, bright pixels indicate qualitative improvement (arterial signal increase). B) Reduction in signal intensity of hybrid data (Fig 3C) vs. base-max data (Fig 3B). Here, dark pixels indicate qualitative improvement (venous signal reduction).

REFERENCES: **1.** Fan Z, Sheehan J, Bi X, Liu X, Carr J, Li D. 3D Magn Reson Med 2009; 62: 1523-1532. **2.** Fan Z, Bi X, Zhou X, Zhuelsdorff S, Dharmakumar R, Carr J, Li D. ISMRM Proceedings 2010; 1307. **3.** Fan Z, Zhang Z, Chung Y-C, Weale P, Zuehlsdorff S, Carr J, Li D. J Magn Reson Imaging 2010; 31: 645-654. **4.** Haacke M, Brown RW, Thompson MR, Venkatesan R. New York: Wiley-Liss; 1999 23: 673-675.